Lattice effective field theory for medium-mass nuclei

CrossMark

Timo A. Lähde [a,*], Evgeny Epelbaum [b], Hermann Krebs [b], Dean Lee [c], Ulf-G. Meißner [a,d,e],
Gautam Rupak [f]

[a] *Institute for Advanced Simulation, Institut für Kernphysik, and Jülich Center for Hadron Physics, Forschungszentrum Jülich, D-52425 Jülich, Germany*
[b] *Institut für Theoretische Physik II, Ruhr-Universität Bochum, D-44870 Bochum, Germany*
[c] *Department of Physics, North Carolina State University, Raleigh, NC 27695, USA*
[d] *Helmholtz-Institut für Strahlen- und Kernphysik and Bethe Center for Theoretical Physics, Universität Bonn, D-53115 Bonn, Germany*
[e] *JARA – High Performance Computing, Forschungszentrum Jülich, D-52425 Jülich, Germany*
[f] *Department of Physics and Astronomy, Mississippi State University, Mississippi State, MS 39762, USA*

A B S T R A C T

We extend Nuclear Lattice Effective Field Theory (NLEFT) to medium-mass nuclei, and present results for the ground states of alpha nuclei from ^{4}He to ^{28}Si, calculated up to next-to-next-to-leading order (NNLO) in the EFT expansion. This computational advance is made possible by extrapolations of lattice data using multiple initial and final states. For our soft two-nucleon interaction, we find that the overall contribution from multi-nucleon forces must change sign from attractive to repulsive with increasing nucleon number. This effect is not produced by three-nucleon forces at NNLO, but it can be approximated by an effective four-nucleon interaction. We discuss the convergence of the EFT expansion and the broad significance of our findings for future *ab initio* calculations.

© 2014 The Authors. Published by Elsevier B.V. This is an open access article under the CC BY license (http://creativecommons.org/licenses/by/3.0/). Funded by SCOAP³.

1. Introduction

Several *ab initio* methods are being used to study nuclear structure. These include coupled-cluster expansions [1], the no-core shell model [2,3], the in-medium similarity renormalization group approach [4], self-consistent Green's functions [5], and Green's function Monte Carlo [6]. The use of soft chiral nuclear EFT interactions has stimulated much of the recent progress in *ab initio* nuclear structure calculations. By "soft" interactions, we refer to the absence of strong repulsive forces at short distances. In this letter, we address a central question in nuclear structure theory: How large a nucleus can be calculated from first principles using the framework of chiral nuclear EFT, and what are the remaining challenges?

We address this question by using Nuclear Lattice Effective Field Theory (NLEFT) to calculate the ground states of alpha nuclei from ^{4}He to ^{28}Si. NLEFT is an *ab initio* method where chiral nuclear EFT is combined with Auxiliary-Field Quantum Monte Carlo (AFQMC) lattice calculations. NLEFT differs from other *ab initio* methods in that it is an unconstrained Monte Carlo calculation, which does not require truncated basis expansions, many-body perturbation theory, or any constraint on the nuclear wave function. Our NLEFT re-

sults are thus truly unbiased Monte Carlo calculations. The results presented here form an important benchmark for *ab initio* calculations of larger nuclei using chiral nuclear EFT. Any deficiencies are indicative of shortcomings in the specific nuclear interactions, rather than of errors generated by the computational method. Such a definitive analysis would be difficult to achieve using other methods.

The lattice formulation of chiral nuclear EFT is described in Ref. [7], a review of lattice EFT methods can be found in Ref. [9], and Refs. [10,11] provide a comprehensive overview of chiral nuclear EFT. We have recently applied NLEFT to describe the structure of the Hoyle state [12,13] and the dependence of the triple-alpha process on the fundamental parameters of nature [14]. These studies show that NLEFT is successful up to $A \simeq 12$ nucleons. In this letter, we report the first NLEFT results for medium-mass nuclei. We compute the ground state energies for all nuclei in the alpha ladder up to ^{28}Si using the lattice action established in Refs. [13, 12,15].

2. Chiral nuclear EFT for medium-mass nuclei

According to chiral nuclear EFT, our calculations are organized in powers of a generic soft scale Q associated with factors of momenta and the pion mass. We label the $\mathcal{O}(Q^0)$ contributions to the nuclear Hamiltonian as leading order (LO), $\mathcal{O}(Q^2)$ as next-to-leading order (NLO), and $\mathcal{O}(Q^3)$ as next-to-next-to-leading order (NNLO)

* Corresponding author.
  E-mail address: t.laehde@fz-juelich.de (T.A. Lähde).

(NNLO). The present calculations are performed up to NNLO. Our LO lattice Hamiltonian includes a significant part of the NLO and higher-order corrections by making use of smeared contact interactions [7,8,15]. See Ref. [15] for a discussion of the interactions used in this work. As discussed in Ref. [15], we are using a low-momentum power counting scheme where there are no additional two-nucleon corrections at NNLO beyond the terms already appearing at NLO.

The NLEFT calculations reported here are performed with a lattice spacing of $a = 1.97$ fm in a periodic cube of length $L = 11.82$ fm. Our trial wave function is denoted $|\Psi_A^{\text{init}}\rangle$, which is a Slater-determinant state composed of delocalized standing waves in the periodic cube, with A nucleons and the desired spin and isospin quantum numbers. For simplicity, we describe our calculations using the language of continuous time evolution. The actual AFQMC calculations use transfer matrices with a temporal lattice spacing of $a_t = 1.32$ fm [9].

Before we enter into the main part of the calculation, we make use of a low-energy filter based upon Wigner's SU(4) symmetry, where the spin–isospin degrees of freedom of the nucleon are all equivalent as four components of an SU(4) multiplet. Let us define

$$H_{\text{SU}(4)} \equiv H_{\text{free}} + \frac{1}{2} C_{\text{SU}(4)} \sum_{\vec{n},\vec{n}'} :\rho(\vec{n}) f(\vec{n} - \vec{n}') \rho(\vec{n}'): , \tag{1}$$

where $f(\vec{n} - \vec{n}')$ is a Gaussian smearing function with width set by the average effective range of the two S-wave interaction channels, and ρ is the total nucleon density. We then apply the exponential of $H_{\text{SU}(4)}$ to obtain

$$|\Psi_A(t')\rangle \equiv \exp(-H_{\text{SU}(4)} t') |\Psi_A^{\text{init}}\rangle, \tag{2}$$

which we refer to as a "trial state". This part of the calculation is computationally inexpensive since it only requires a single auxiliary field and does not generate any sign oscillations in the Monte Carlo calculation.

Next, we use the LO Hamiltonian H_{LO} to construct the Euclidean-time projection amplitude

$$Z_A(t) \equiv \langle \Psi_A(t') | \exp(-H_{\text{LO}} t) | \Psi_A(t') \rangle, \tag{3}$$

from which we compute the "transient energy"

$$E_A(t) = -\partial [\ln Z_A(t)] / \partial t. \tag{4}$$

If the lowest eigenstate of H_{LO} that possesses a non-vanishing overlap with the trial state $|\Psi_A(t')\rangle$ is denoted $|\Psi_{A,0}\rangle$, the energy $E_{A,0}$ of $|\Psi_{A,0}\rangle$ is obtained as the $t \to \infty$ limit of $E_A(t)$.

The higher-order corrections to $E_{A,0}$ are evaluated using perturbation theory. We compute expectation values using

$$\begin{aligned} Z_A^{\mathcal{O}}(t) &\equiv \langle \Psi_A(t') | \exp(-H_{\text{LO}} t/2) \\ &\quad \times \mathcal{O} \exp(-H_{\text{LO}} t/2) | \Psi_A(t') \rangle, \end{aligned} \tag{5}$$

for any operator $\mathcal{O}$. Given the ratio

$$X_A^{\mathcal{O}}(t) = Z_A^{\mathcal{O}}(t) / Z_A(t), \tag{6}$$

the expectation value of $\mathcal{O}$ for the desired state $|\Psi_{A,0}\rangle$ is again obtained in the $t \to \infty$ limit according to

$$X_{A,0}^{\mathcal{O}} \equiv \langle \Psi_{A,0} | \mathcal{O} | \Psi_{A,0} \rangle = \lim_{t \to \infty} X_A^{\mathcal{O}}(t), \tag{7}$$

which gives the corrections to $E_{A,0}$ induced by the NLO and NNLO contributions.

The closer $|\Psi_A(t')\rangle$ is to $|\Psi_{A,0}\rangle$, the less the required projection time t. The trial state can be optimized by adjusting both the SU(4) projection time t' and the strength of the coupling $C_{\text{SU}(4)}$ of $H_{\text{SU}(4)}$. Here, we show that the accuracy of the extrapolation

$t \to \infty$ can be further improved by simultaneously incorporating data from multiple trial states that differ in the choice of $C_{\text{SU}(4)}$. This approach enables a "triangulation" of the asymptotic behavior as the common limit of several different functions of t.

3. Extrapolation in Euclidean time

The behavior of $Z_A(t)$ and $Z_A^{\mathcal{O}}(t)$ at large t is controlled by the low-energy spectrum of H_{LO}. Let $|E\rangle$ label the eigenstates of H_{LO} with energy E, and let $\rho_A(E)$ denote the density of states for a system of A nucleons. For simplicity, we omit additional labels needed to distinguish degenerate states. We can then express $Z_A(t)$ and $Z_A^{\mathcal{O}}(t)$ in terms of their spectral representations,

$$Z_A(t) = \int dE \, \rho_A(E) \big| \langle E | \Psi_A(t') \rangle \big|^2 \exp(-Et), \tag{8}$$

$$\begin{aligned} Z_A^{\mathcal{O}}(t) &= \int dE \, dE' \, \rho_A(E) \rho_A(E') \exp\big(-(E + E')t/2\big), \\ &\quad \times \langle \Psi_A(t') | E \rangle \langle E | \mathcal{O} | E' \rangle \langle E' | \Psi_A(t') \rangle, \end{aligned} \tag{9}$$

from which the spectral representations of $E_A(t)$ and $X_A^{\mathcal{O}}(t)$ are obtained using Eq. (4) and Eq. (6), respectively. We can approximate these to arbitrary accuracy over any finite range of t by taking $\rho_A(E)$ to be a sum of energy delta functions,

$$\rho_A(E) \approx \sum_{i=0}^{i_{\max}} c_i \delta(E - E_{A,i}), \tag{10}$$

where we use $i_{\max} = 4$ for the calculation of the ^{4}He ground state, and $i_{\max} = 3$ for $A \geqslant 8$. These choices give a good description over the full range of t for all trial states, without introducing too many free parameters. Using AFQMC data for different values of $C_{\text{SU}(4)}$, we perform a correlated fit of $E_A(t)$ and $X_A^{\mathcal{O}}(t)$ for all operators $\mathcal{O}$ that contribute to the NLO and NNLO corrections. We find that using 2–6 distinct trial states for each A allows for a much more precise determination of $E_{A,0}$ and $X_{A,0}^{\mathcal{O}}$ than hitherto possible. In particular, we may "triangulate" $X_{A,0}^{\mathcal{O}}$ using trial states that correspond to functions $X_A^{\mathcal{O}}(t)$ which converge both from above and below.

As the extent of our MC data in Euclidean time is relatively short, we discuss next the level of confidence that we can attribute to our results. In our "triangulation" method, the accuracy and reliability of the extrapolation $t \to \infty$ is increased by means of correlated fits to multiple trial states. We first note that the number of Euclidean time steps N_t available for the extrapolation does not decrease drastically with the number of nucleons A. This inspires confidence that our method, which has by now been successfully applied to the structure, spectrum and electromagnetic properties of ^{16}O in Ref. [16] should also be applicable to heavier systems. Nevertheless, "spurious early convergence" in Euclidean time extrapolations should be carefully guarded against. If only one trial state is used, this issue arises much more readily. In our "triangulation" method, the extrapolation is very strongly constrained by the requirement that all observables for all trial states should be described by the same exponential dependence on Euclidean time. Rapid convergence in t then translates into a small sensitivity to $C_{\text{SU}(4)}$ at large values of t. It is also encouraging to note that our new extrapolations are consistent with our earlier results for ^{12}C in Refs. [13,14], which were computed using delocalized plane-wave as well as alpha-cluster trial wave functions.

4. Lattice Monte Carlo results

In Fig. 1, we show the LO transient energy $E_A(t)$ as a function of the number of temporal lattice steps $N_t = t/a_t$, for ^{16}O
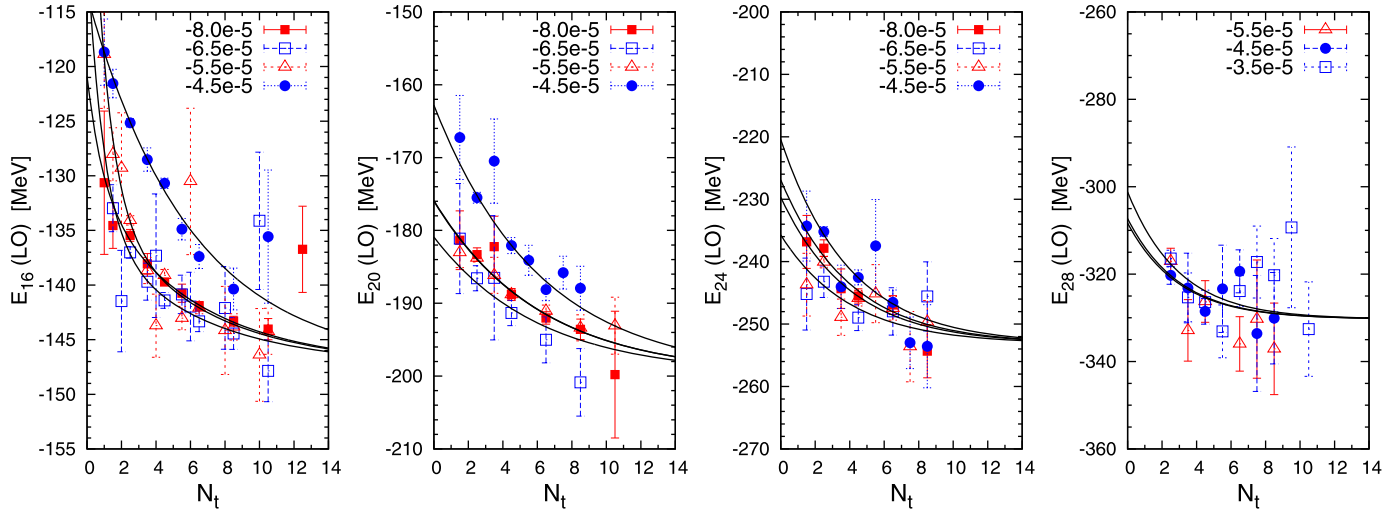
Fig. 1. NLEFT results for the LO transient energy $E_A(t)$ for $A = 16$ to $A = 28$, with $C_{SU(4)}$ given (in MeV^{-2}) for each trial state. The curves show a fit using a spectral density $\rho_A(E)$ given by a sum of three energy delta functions. The fits for $E_A(t)$ are correlated with those of Figs. 2 and 3.
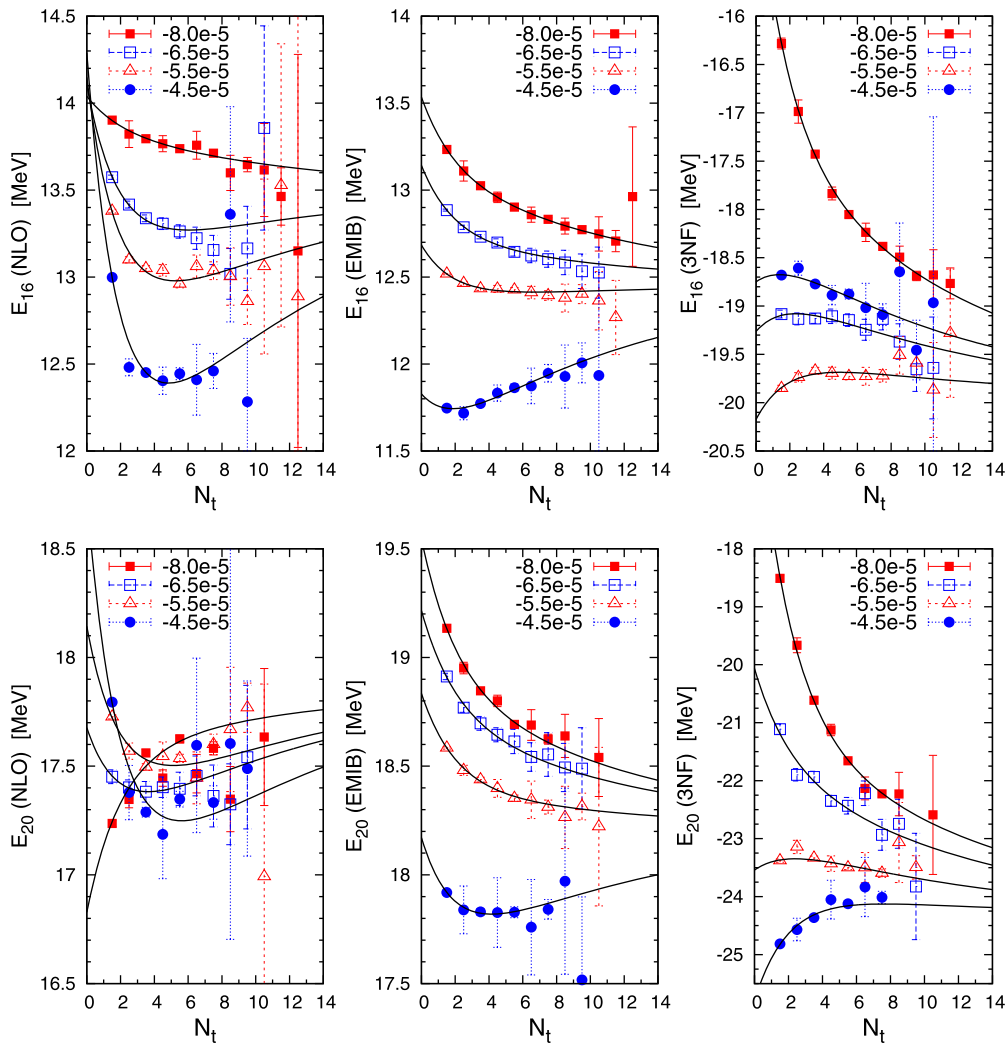

Fig. 2. NLEFT results for the matrix elements $X_A^{\mathcal{O}}(t)$ for $A = 16$ and $A = 20$, with $C_{SU(4)}$ given (in MeV^{-2}) for each trial state. The left panels show the total isospin-symmetric NLO correction, the central panels the electromagnetic and isospin-breaking (EMIB) corrections, and the right panels the total three-nucleon force (3NF) correction. The curves show a fit with $\rho_A(E)$ given by the sum of three energy delta functions, correlated with those of Fig. 1.
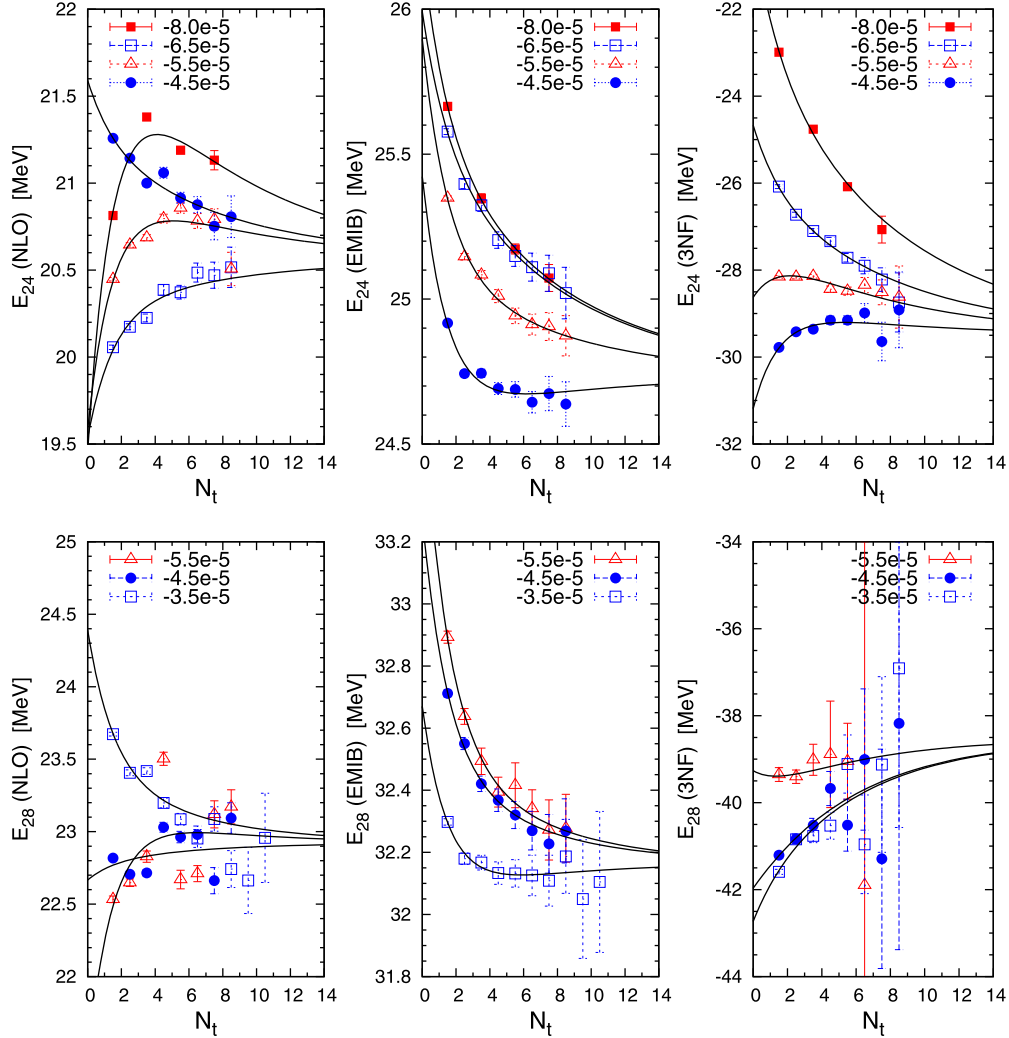
Fig. 3. NLEFT results for the matrix elements $X_A^{\mathcal{O}}(t)$ for $A = 24$ and $A = 28$. The notation is as for Fig. 2.

through ^{28}Si. The curves show a simultaneous fit to all trial states employed, with $\rho_A(E)$ given by a sum of three energy delta functions. In Figs. 2 and 3, we similarly show the expectation values $X_A^{\mathcal{O}}(t)$ for ^{16}O through ^{24}Mg. These include the sum of isospin-symmetric NLO corrections (NLO), the sum of the electromagnetic and strong isospin-breaking corrections (EMIB), and the total three-nucleon force contribution (3NF) which first appears at NNLO. It should be noted that the fits shown in Fig. 1 are correlated with those of Figs. 2 and 3, and use the same spectral density $\rho_A(E)$. Moreover, each of the $\simeq 30$ contributions $X_A^{\mathcal{O}}(t)$ to the NLO, EMIB and 3NF corrections is individually accounted for in the analysis. We also emphasize that the fits for each A are independent.

Our NLEFT results for the alpha nuclei from ^{4}He to ^{28}Si are summarized in Table 1, with statistical and extrapolation uncertainties shown in parentheses. For comparison, we also show the empirical ground-state energies. The LO energies are given in the second column of Table 1, while the third column shows the results using the two-nucleon force up to NNLO. Our "LO" calculations are actually improved LO calculations with smeared short-range interactions that capture a significant portion of the corrections usually treated at NLO [7]. The fourth column includes the 3NF at NNLO. As discussed in Ref. [8], the local 3N contact interaction induces significant lattice artifacts when acting on configurations of four nucleons at the same lattice site. Following Ref. [8],

we have removed this systematic effect by subtraction of a local 4N contact interaction. In the column labeled "+3N" in Table 1, the strength of this subtraction has been set to reproduce the empirical binding energy of ^{8}Be. We have not yet included systematic errors due to the finite-volume effects in a box of size $L = 11.8$ fm, but preliminary results at larger volumes are suggestive of a $\sim$1% reduction in the binding of each nucleus in the infinite-volume limit. In particular, we expect that $\sim$50% of the observed $\simeq 0.7$ MeV overbinding of ^{4}He should vanish.

Our NNLO results with the 3NF included appear to be within a few percent of the empirical energies for $A \leqslant 12$, while for ^{16}O we find an overbinding of $\simeq 9$%. Such an accuracy is, by itself, reasonably good for a calculation which is truncated at NNLO at a lattice spacing of $a = 1.97$ fm. However, for ^{20}Ne the observed overbinding increases to $\simeq 15$%, for ^{24}Mg to $\simeq 17$%, and for ^{28}Si it reaches $\simeq 30$%. It is thus clearly a systematical effect. In this context, we note that other *ab initio* methods using soft potentials encounter similar problems in the description of both light and medium-mass nuclei using the same set of interactions [1–3].

Before we discuss the challenge of resolving this overbinding problem in future *ab initio* calculations, it is useful to explore the nature of the missing physics in the present work. As we ascend the alpha ladder from ^{4}He to ^{28}Si, the lighter nuclei can be described as collections of alpha clusters [13,12]. As the number of

Table 1

NLEFT results for the ground-state energies (in MeV). The combined statistical and extrapolation errors are given in parentheses. The columns labeled "LO (2N)" and "NNLO (2N)" show the energies at each order using the two-nucleon force only. The column labeled "+3N" also includes the 3NF, which first appears at NNLO. Finally, the column "+4N$_{\text{eff}}$" includes the effective 4N contribution from Eq. (11). The column "Exp" gives the empirical energies.

A	LO (2N)	NNLO (2N)	+3N	+4N$_{\text{eff}}$	Exp
4	−28.87(6)	−25.60(6)	−28.93(7)	−28.93(7)	−28.30
8	−57.9(1)	−48.6(1)	−56.4(2)	−56.3(2)	−56.35
12	−96.9(2)	−78.7(2)	−91.7(2)	−90.3(2)	−92.16
16	−147.3(5)	−121.4(5)	−138.8(5)	−131.3(5)	−127.62
20	−199.7(9)	−163.6(9)	−184.3(9)	−165.9(9)	−160.64
24	−253(2)	−208(2)	−232(2)	−198(2)	−198.26
28	−330(3)	−275(3)	−308(3)	−233(3)	−236.54

clusters increases, they become increasingly densely packed, such that a more uniform liquid of nucleons is approached. This increase in the density of alpha clusters appears correlated with the gradual overbinding we observe at NNLO for $A \geqslant 16$. As this effect becomes noticeable for ^{16}O, we can view it as a problem which first arises in a system of four alpha clusters. The alpha-cluster structure of ^{16}O will be discussed in more detail in a forthcoming publication [16]. Following Ref. [8], which removed discretization errors associated with four nucleons occupying the same lattice site, we can attempt to remove similar errors associated with four alpha clusters in close proximity on neighboring lattice sites. The simplest interaction which permits a removal of the overbinding associated with such configurations is

$$V^{(4N_{\text{eff}})} = D^{(4N_{\text{eff}})} \sum_{1 \leqslant (\vec{n}_i - \vec{n}_j)^2 \leqslant 2} \rho(\vec{n}_1)\rho(\vec{n}_2)\rho(\vec{n}_3)\rho(\vec{n}_4), \quad (11)$$

with $\rho(\vec{n})$ the total nucleon density. The summation includes nearest or next-to-nearest neighbor (spatial) lattice sites.

In Table 1, the column labeled "+4N$_{\text{eff}}$" shows the results at NNLO while including both the 3NF and $V^{(4N_{\text{eff}})}$. Due to the low momentum cutoff, the two-pion exchange contributions have been absorbed into the contact interactions at NLO. We have tuned $D^{(4N_{\text{eff}})}$ to give approximately the correct energy for the ground state of ^{24}Mg. With $V^{(4N_{\text{eff}})}$ included, a good description of the ground-state energies is obtained over the full range from light to medium-mass nuclei, with a maximum error no larger than ∼3%. This lends support to the qualitative picture that the overbinding of the NNLO results in Table 1 is associated with the increased packing of alpha clusters and the eventual crossover to a uniform nucleon liquid. The missing physics would then be comprised of short-range repulsive forces that counteract the dense packing of alpha clusters.

In spite of the good agreement with experiment in Table 1 upon introduction of $V^{(4N_{\text{eff}})}$, we also need to consider whether this could be merely an accidental effect. It is then helpful to check whether a consistent picture is obtained with respect to excited states, transitions and electromagnetic properties of the nuclei in the medium-mass range where $V^{(4N_{\text{eff}})}$ gives a sizable contribution. In Ref. [16], we find very convincing evidence supporting our results and analysis from the properties of ^{16}O, including its first excited 0^+ state. In particular, the excitation energies and level ordering in ^{16}O was found to be very sensitive to the strength and form of $V^{(4N_{\text{eff}})}$. Such a sensitivity arises due to the differences in the alpha-cluster structure of the states in question.

The coefficient of $V^{(4N_{\text{eff}})}$ can be expressed as $D^{(4N_{\text{eff}})} = 0.9/(f_\pi^7 \Lambda_\chi)$, where we use $f_\pi = 92.4$ MeV and $\Lambda_\chi = 700$ MeV as in Ref. [17]. While the magnitude of $D^{(4N_{\text{eff}})}$ appears to be somewhat large compared to what is expected based on naive dimensional analysis, the effective 4N contribution to *e.g.* the alpha particle binding energy is negligibly small, in agreement with

the chiral power counting. Thus, the increasing effective 4N contributions that we find for $A \geqslant 16$ are the result of large operator expectation values for the nuclear wave function. We expect that this effect is due to the coarse lattice spacing, and can be ameliorated by using a smaller lattice spacing and an interaction with more short-range repulsion.

5. Conclusions

Let us now return to the question we posed at the beginning: How large a nucleus can be calculated from first principles using chiral nuclear EFT, and what are the remaining challenges? Using a soft nucleon–nucleon interaction with a momentum cutoff scale of $\pi/a \simeq 314$ MeV, we found that the two-nucleon potential is accurate for lighter nuclei but overbinds those beyond ^{16}O. As a result, the overall contribution of multi-nucleon forces must compensate by changing sign from attractive to repulsive with increasing A. While such an effect cannot be accommodated by the 3NF at NNLO alone, the overall contribution from higher-order interactions should be similar to our effective four-nucleon interaction, which counteracts the packing of alpha clusters. Still, this implies a large correction from higher-order terms. Analogous problems will arise in computational methods that use renormalization group flows to soften the two-nucleon interaction. In that case, the large repulsive corrections appear in the form of strong induced multi-nucleon forces.

From our analysis, the path forward for *ab initio* calculations of heavier nuclei using chiral nuclear EFT appears clear. The softening of the two-nucleon interaction should not be pushed so far that heavier nuclei become significantly overbound by the two-nucleon force alone. This is not merely an issue for NLEFT, but would appear to be a universal criterion for all *ab initio* methods. A concerted effort should be made to improve the current computational algorithms to handle interactions with more short-range repulsion. The NLEFT collaboration is now exploring this approach for studies of larger nuclei. We are now in the process of improving the lattice algorithms for calculations at smaller lattice spacings, and extending NLEFT to N^{3}LO in the chiral expansion.

References

[1] G. Hagen, M. Hjorth-Jensen, G.R. Jansen, R. Machleidt, T. Papenbrock, Phys. Rev. Lett. 109 (2012) 032502.
[2] E.D. Jurgenson, P. Maris, R.J. Furnstahl, P. Navratil, W.E. Ormand, J.P. Vary, Phys. Rev. C 87 (2013) 054312.
[3] R. Roth, J. Langhammer, A. Calci, S. Binder, P. Navratil, Phys. Rev. Lett. 107 (2011) 072501.
[4] H. Hergert, S.K. Bogner, S. Binder, A. Calci, J. Langhammer, R. Roth, A. Schwenk, Phys. Rev. C 87 (2013) 034307.
[5] V. Soma, C. Barbieri, T. Duguet, Phys. Rev. C 87 (2013) 011303.
[6] A. Lovato, et al., Phys. Rev. Lett. 111 (2013) 092501.
[7] B. Borasoy, E. Epelbaum, H. Krebs, D. Lee, Ulf-G. Meißner, Eur. Phys. J. A 31 (2007) 105.

[8] E. Epelbaum, H. Krebs, D. Lee, Ulf-G. Meißner, Phys. Rev. Lett. 104 (2010) 142501;
E. Epelbaum, H. Krebs, D. Lee, Ulf-G. Meißner, Eur. Phys. J. A 45 (2010) 335.
[9] D. Lee, Prog. Part. Nucl. Phys. 63 (2009) 117.
[10] E. Epelbaum, H.-W. Hammer, Ulf-G. Meißner, Rev. Mod. Phys. 81 (2009) 1773.
[11] R. Machleidt, D.R. Entem, Phys. Rep. 503 (2011) 1.
[12] E. Epelbaum, H. Krebs, D. Lee, Ulf-G. Meißner, Phys. Rev. Lett. 106 (2011) 192501.
[13] E. Epelbaum, H. Krebs, T.A. Lähde, D. Lee, Ulf-G. Meißner, Phys. Rev. Lett. 109 (2012) 252501.
[14] E. Epelbaum, H. Krebs, T.A. Lähde, D. Lee, Ulf-G. Meißner, Phys. Rev. Lett. 110 (2013) 112502;
E. Epelbaum, H. Krebs, T.A. Lähde, D. Lee, Ulf-G. Meißner, Eur. Phys. J. A 49 (2013) 82.
[15] E. Epelbaum, H. Krebs, D. Lee, Ulf-G. Meißner, Eur. Phys. J. A 41 (2009) 125.
[16] E. Epelbaum, H. Krebs, T.A. Lähde, D. Lee, Ulf-G. Meißner, G. Rupak, Phys. Rev. Lett. 112 (2014) 102501, arXiv:1312.7703 [nucl-th].
[17] E. Epelbaum, A. Nogga, W. Glöckle, H. Kamada, Ulf-G. Meißner, H. Witała, Phys. Rev. C 66 (2002) 064001.